



This is a repository copy of *Effects of tool coating and tool wear on the surface quality and flexural strength of slotted CFRP*.

White Rose Research Online URL for this paper:  
<https://eprints.whiterose.ac.uk/185818/>

Version: Published Version

---

**Article:**

Ashworth, S., Fairclough, J.P.A. [orcid.org/0000-0002-1675-5219](https://orcid.org/0000-0002-1675-5219), Meredith, J. et al. (2 more authors) (2022) Effects of tool coating and tool wear on the surface quality and flexural strength of slotted CFRP. *Wear*, 498-499. 204340. ISSN 0043-1648

<https://doi.org/10.1016/j.wear.2022.204340>

---

**Reuse**

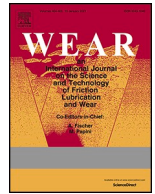
This article is distributed under the terms of the Creative Commons Attribution (CC BY) licence. This licence allows you to distribute, remix, tweak, and build upon the work, even commercially, as long as you credit the authors for the original work. More information and the full terms of the licence here:  
<https://creativecommons.org/licenses/>

**Takedown**

If you consider content in White Rose Research Online to be in breach of UK law, please notify us by emailing [eprints@whiterose.ac.uk](mailto:eprints@whiterose.ac.uk) including the URL of the record and the reason for the withdrawal request.



[eprints@whiterose.ac.uk](mailto:eprints@whiterose.ac.uk)  
<https://eprints.whiterose.ac.uk/>



# Effects of tool coating and tool wear on the surface quality and flexural strength of slotted CFRP

Sam Ashworth<sup>a,\*</sup>, J. Patrick A. Fairclough<sup>b</sup>, James Meredith<sup>c</sup>, Yoshihiro Takikawa<sup>d</sup>, Kevin Kerrigan<sup>e</sup>

<sup>a</sup> Industrial Doctorate Centre in Machining Science, Advanced Manufacturing Research Centre with Boeing, University of Sheffield, Rotherham, S60 5TZ, UK

<sup>b</sup> Department of Mechanical Engineering, University of Sheffield, Sir Frederick Mappin Building, Mappin Street, Sheffield, S1 3JD, UK

<sup>c</sup> WMG, International Manufacturing Centre, University of Warwick, Coventry, CV4 7AL, UK

<sup>d</sup> OSG Corporation, 3-22 Honnoghara, Toyokawa, Aichi, 442-8543, Japan

<sup>e</sup> Advanced Manufacturing Research Centre with Boeing, The University of Sheffield, Advanced Manufacturing Park, Wallis Way, Catcliffe, Rotherham, S60 5TZ, UK

## ARTICLE INFO

### Keywords:

Cutting tools  
Polymer-matrix composite  
CVD coatings  
Surface analysis

## ABSTRACT

Machining of carbon fibre reinforced polymer (CFRP) is abrasive and causes significant tool wear. The effect of tool wear on static flexural strength is investigated, using edge trimming with uncoated carbide and chemical vapour deposition (CVD) diamond coated burr style tools. Edge rounding (*ER*) criteria along with flank wear are used to observe tool degradation with *ER* shown to preferentially wear allowing the tool to become cyclically sharper and duller, corresponding to fluctuating dynamometer readings, a novelty for CFRP machining. Areal surface metrics degraded for an uncoated tool due to changes in cutting mechanism, whilst for up to 16.2 m of linear traverse, the coated tool showed limited changes. Tool wear, caused by edge trimming 7.2 m of CFRP, using an uncoated carbide tool, provided a flexural strength reduction of up to 10.5 %, directly linking tool wear to reduced mechanical strength.

## 1. Introduction

CFRP materials see ever increasing using in the aerospace industry [1] due to its high specific strength to weight ratio [2]. Machining of CFRP material is required to achieve final net shape and is notoriously harsh on cutting tools due to the anisotropic, abrasive nature of fibre, causing tool wear. Relatively little, if any, plastic deformation occurs in front of the tool cutting edge for thermoset CFRP and fibres are directly exposed at the cutting interface [3] which exacerbates tool wear. Tool wear in the form of edge acuity reduction over time is an important aspect of machining due to the increase of cutting forces associated with worn tools and subsequent degradation of surface quality [4–7]. The link of worn tools to CFRP surface quality degradation has been rarely explored [3,8], especially for edge trimming operations using areal metrics.

The wear of tools from CFRP specific machining processes needs careful consideration due to the anisotropic and harsh frictional characteristics of CFRP [9]. Various tool substrates and coatings have been designed to overcome the issue of high tool wear such as carbides, cemented carbides, coated carbides, ceramics, PCBN and PCD [10,11].

Whilst most literature covers carbide and PCD tooling effects on material surface quality, limited literature exists for CVD diamond coated tools, especially for edge milling tool wear trials, where CVD is currently rated as the most hard and durable cutting edge tool type by manufacturers [12].

Standards exist for the measurement of tool wear which primarily focus on flank wear,  $V_B$ , as a measure of tool life [13]. However,  $V_B$  may not be a suitable metric to measure tool wear due to the unique cutting mechanism and wear that occurs in the machining of CFRP. To this end Faraz, Biermann and Weinert [14] created a new metric for measuring tool wear during the drilling of CFRP material which focused on the cutting edge radius, *ER*. Whilst successfully trialled on drilling [11,14] and orthogonal edge trimming tools [15–17], *ER* can be applied to more complex tooling such as burr style routers.

Significant work has been completed to assess machining variables that alter CFRP surface quality. Many variables exist which influence surface quality such as temperature [18,19], machine parameters [20, 21], changes in feed and cutting speed parameters [19,22] and tool geometry [23]. Increased temperature in the cutting zone can adversely affect the surface quality [18]. However, this effect is linked with other

\* Corresponding author.

E-mail address: [s.o.ashworth@salford.ac.uk](mailto:s.o.ashworth@salford.ac.uk) (S. Ashworth).

<https://doi.org/10.1016/j.wear.2022.204340>

Received 1 September 2021; Received in revised form 21 February 2022; Accepted 1 April 2022

Available online 4 April 2022

0043-1648/© 2022 The Authors. Published by Elsevier B.V. This is an open access article under the CC BY license (<http://creativecommons.org/licenses/by/4.0/>).

variables. Haddad et al. [19] showed that thermal damage on the trimmed edge of CFRP increases with greater cutting speed and that worn tools were the cause of more thermal damage, measured by scanning electron microscope (SEM). Sheikh-Ahmad and Shahid [22] note similar trends with  $R_a$  and  $R_z$  2D surface metric verification. In addition to the aforementioned variables, cutting edge radius has also been studied within literature. Tool coating was assessed by Haddad et al. [23] who showed that uncoated tools produced surfaces of lower  $R_a$  than coated counterparts. Tool wear and edge radius of orthogonal machining of CFRP has been studied by Duboust et al. [15] showing that cutting forces increased with larger ER, as anticipated due to large contact area and friction. Further studies show that the ER change and subsequent increase in cutting forces adversely affects the surface in terms of areal metrics  $S_a$  and  $S_v$  [16] and delamination [17]. This is in agreement with Nguyen-Dinh et al. [24] who also use 3D metrics to show increasing forces and surface damage with increased tool wear but go further to suggest that crater volume is the critical measurement metric. Wang et al. [25] note that the ER of the tool is critical, in particular when fibre angle is less than  $90^\circ$  which is present in most laminate structures. However, of the ER and tool wear studies completed, none have linked directly to mechanical performance.

Mechanical performance has been assessed and linked to surface quality for some machining variables. Of the variables assessed, such as feed speed [22], machine setup parameters [19–21,26,27], it is noted that changes in the surface properties alter mechanical performance. A range of metrics have been used to determine the surface quality, with crater depth found to be effective [26–28], however a full range of areal metrics has not been analysed to determine if conventional criteria are adequate. Whilst tool wear phenomena has been observed for CFRP machining and linked to surface quality, as previously noted [3,8,15,25], little evidence exists for the correlation of tool wear metrics to dynamometer readings of cutting forces, surface integrity and/or final mechanical performance of the trimmed samples. This could have significant consequences, for example, if no link were found, industry could move away from the current approach of applying a conservative tool life which results in high tooling expenditure. The use of finishing milling, whereby the material is given a final cutting pass by a finishing tool (e.g. DIA-MFC provided by OSG Corp.), could also be removed from the process, saving time and money. Conversely, if tool wear does have an impact on mechanical performance, upper limits on surface quality and links to tool life could be applied.

In this experimental study, the link between tool wear, surface quality and final mechanical performance of trimmed samples is explored. Tool wear, measured using traditional ( $V_B$ ) and CFRP specific (ER) metrics, for uncoated and CVD coated carbide burr style edge trimming tools, is determined at high regularity, alongside the corresponding surface quality metrics of the trimmed material. The range of previous studies shows that surface quality has been measured in 2D and 3D contact and non-contact methods alongside SEM and visual observations. 3D areal surface quality, in terms of spatial and volumetric parameter metrics, will be used to fully capture machined surface integrity. Mechanical performance, to determine strength changes caused by tool wear and surface quality which has previously not been explored directly in literature, will be assessed by four-point-bending flexural strength tests.

## 2. Material and methods

### 2.1. CFRP panel manufacture and characterisation

5 off 300 x 300 x 3 mm CFRP panels with a [(0/90)<sub>F</sub>, (±45)<sub>F,3</sub>, (0/90)<sub>F</sub>]<sub>S</sub> layup, a T300, 2x2 material (Sigmatex, UK), DGEFB PY306 epoxy (Huntsman, UK) and a TETA hardener (Sigma Aldrich, UK) were manufactured as described in authors previous work [20].

The manufactured panels were processed using differential scanning calorimetry (DSC), dynamic mechanical analysis (DMA) and optical

microscopy to determine degree of cure,  $\tan \delta$  glass transition temperature ( $T_g$ ) and void quantity, respectively.

A PerkinElmer Diamond DSC machine was used to determine degree of cure using change in enthalpy ( $\Delta h$ ) between uncured and cured systems, in order to ensure similar levels of cross linking between the 8 manufactured panels. Resin samples placed in DSC pans alongside each 300 x 300 x 3 mm panel during cure. Uncured and cured resin samples were heated from 30 to 300 °C at 10 °C/min to determine  $\Delta h$ .

A PerkinElmer DMA800 machine was used to determine a  $\tan \delta T_g$  value. As cutting temperature approaches  $T_g$ , the matrix softens and no longer supports the shearing cutting mechanism of sub- $T_g$  machining [18,29]. If panels were not of the same or similar composition, they may have different  $T_g$  onset temperatures which would significantly change the tool wear mechanics. Therefore, testing the onset  $T_g$  of the 8 manufactured panels used within the wear trials is critical to ensure wear is independent of any manufacturing variations. A 3-point bend test using a 17.5 mm free length, a width of 5 mm and a thickness of 3 mm was used at a ramp rate of 2 °C/min up to a maximum of 160 °C at a frequency of 1 Hz.

A sample of each panel was sectioned using a diamond disc saw and mounted in Epocolor resin (Buehler, UK), cured and polished as per Ashworth et al. [30] recommendations. Image-J (NIH Image, USA) grey scale image segmentation methods were used to determine void content of full thickness images obtained through a 5 MP Paxcam camera mounted in a Qioptiq Fusion optical system (Best Scientific, UK). 5 images per panel were used to determine void content.

### 2.2. Milling equipment

#### 2.2.1. Milling machine tool

A MAG Cincinnati, 3 axis machine tool (see supplementary information) with a BT-40 spindle, a 392.41014-63 40 120B tool holder (Sandvik Coromant, UK) and an ER collet were used to hold milling tools.

#### 2.2.2. Milling fixture

A custom milling fixture, shown in Fig. 1, was used to generate flexural specimens using a full slotting strategy where the tool could pass each side of an aluminium L-bracket (to minimise any workpiece deflection) in a conventional/up milling style. The resulting strips of CFRP material beneath the brackets were then trimmed to flexural specimen lengths using a diamond disc saw to provide 4 samples per strip, 36 samples per panel. See Supplementary Material for video file of cutting process.

Supplementary video related to this article can be found at <https://doi.org/10.1016/j.wear.2022.204340>

#### 2.2.3. Milling tools

A diamond coated carbide (DIA-BNC) and uncoated version (BNC) of the same tool geometry were provided by OSG Corp, Fig. 2. DIA-BNC is a double helix, fine nicked router specifically for CFRP trimming with the geometry designed to eliminate uncut fibres and delamination [12]. The uncoated, exposed tungsten-carbide version was used to exacerbate the effects of tool wear.

The cutting parameters in Table 1 were used throughout the wear trial for both cutting tools at a spindle speed of 8000 RPM which was confirmed through fast fourier transform (FFT) of dynamometer data for all test runs (8000 ± 4 RPM).

#### 2.2.4. Wear assessment protocol

DIA-BNC and BNC tools were inspected using focus variation methods as per the cadence in Table 2 to observe ER and  $V_B$  criteria shown in Fig. 3.  $\Delta ER$  and  $\Delta V_B$  were observed by subtracting unworn,  $ER_{New}$  and  $V_{B,New}$  values. No tooth chipping was observed throughout the trials which would have significantly altered wear, dynamometer, surface property and mechanical performance.

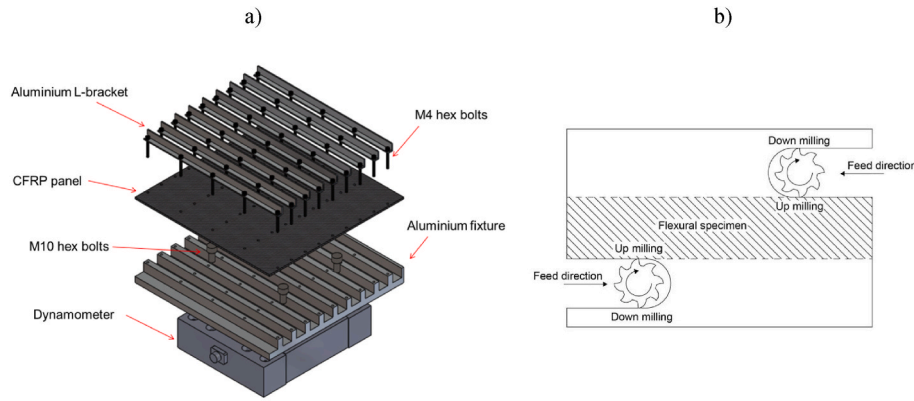


Fig. 1. a) milling fixture layout and b) cutting strategy for generation of flexural specimens.



Fig. 2. a) DIA-BNC and b) uncoated BNC, Ø 6 mm tools.

Table 1

Cutting parameters.

Tool	No. Teeth	Tool diameter (mm)	Cutting speed, $V_c$ (m/min)	FPT, $F_t$ (mm/tooth)	Feed per revolution, $F_N$ (mm/rev)
DIA-BNC/BNC	8	6	150.80	0.015	0.12

Table 2

Tool wear inspection cadence.

Inspection cadence (mm)	Tool
0	DIA-BNC/BNC
1.2	DIA-BNC/BNC
2.4	DIA-BNC/BNC
3.6	DIA-BNC/BNC
4.8	DIA-BNC/BNC
7.2	DIA-BNC/BNC
9.0	DIA-BNC only
11.4	DIA-BNC only
16.2	DIA-BNC only

Focus variation measurements were taken with an Alicona G5 (Bruker, GmbH) using 10x magnification at the same section of tool for each of the noted cutting distances using settings given in Table 3. This resulted in two fully observable teeth, at 0 and 180° tool positions which allows readings to account for any tool dynamic or run-out effects, where run-out was measured below 5 μm each time the tool was inserted into the tool holder. 3 measurements of  $ER$  and  $V_B$  were taken per tooth at 9.4, 9.5 and 9.6 mm from the tip of the tool ( $\pm 0.1$  μm, determined through stage movement calibration checks). Average data with  $\pm 1$  standard deviation are presented in results for all tool wear data.

### 2.2.5. Dynamometer

A Kistler 9139AA plate dynamometer, set to a sampling rate of 20 kHz and a 0–1 kN measuring range, was used to capture cutting forces data during cut at the same inspection cadence as tool wear. The dynamometer was connected to a Kistler 5070A12100 8 channel charge amplifier and DAQ system with Dynoware used to capture cutting forces. Further to this, raw data was compensated for drift and processed to provide data in the form of  $U_T$  using a Matlab script.

$U_T$  has been used as a convenient metric [18,20], which not only captures all cutting forces  $F_x$ ,  $F_y$  and  $F_z$  but relates to volumetric material removal, shown in Equation (1). Where  $F$  is the cutting force,  $x$  is the linear distance milled and  $V$  is the volume of material removed. When the calibrated equipment and volumetric measurements are compounded,  $U_T$  has an uncertainty of  $\pm 0.93\%$  which is applied to all presented  $U_T$  results. Error bars in x-axis data is presented to show measurement points before and after tool wear inspection point ( $\pm 0.225$  m).

$$U_T = \frac{\int F_x dx + \int F_y dx + \int F_z dx}{V} \quad (1)$$

### 2.3. Post machining assessment

#### 2.3.1. Focus variation assessment

Areal surface scanning was conducted by an Alicona G5 focus vari-

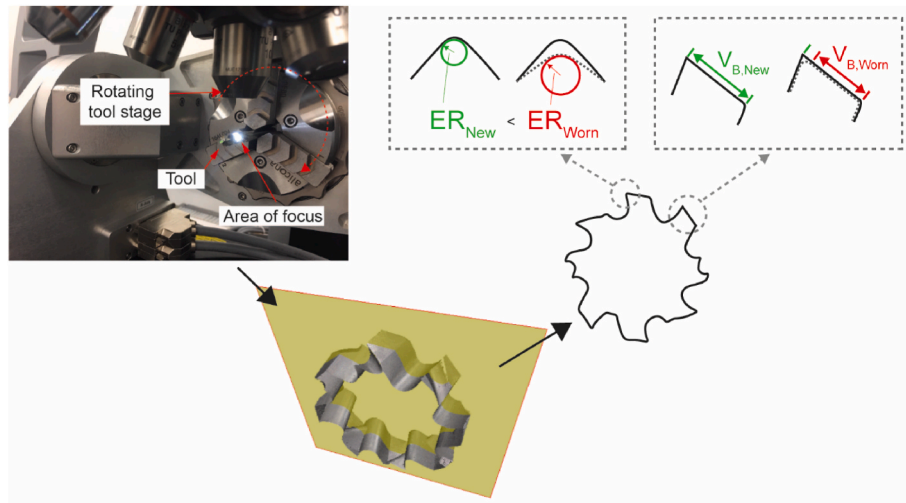


Fig. 3. Alicona G5 rotating tool stage, DIA-BNC 360° tool scan, resulting circumferential profile and associated example tool wear criteria.

Table 3

Focus variation parameters for Alicona tool scans.

Tool	Exposure ( $\mu\text{m}$ )	Contrast	Vertical resolution ( $\mu\text{m}$ )	Lateral resolution ( $\mu\text{m}$ )
DIA-BNC	150	0.36	1	2
BNC	117	0.3	1	2

ation system using 10x magnification on a  $5 \times 3$  mm (full thickness) area with exposure set to 7.25 ms and contrast set to 0.7 using robust Gaussian filtration, providing a repeatability of  $\pm 0.030 \mu\text{m}$ . A  $\lambda_c$  cut-off wavelength of 0.8 mm was used to remove form and waviness from volumetric, spatial, bearing area and autocorrelation metrics. Areal scanning, located at the expected point of flexural failure, Fig. 4, was conducted on 2 flexural samples before and after the tool wear inspection point given in Table 2. Observations were made on each side of the sample resulting in 8 values to correspond with each tool wear inspection point. Average data and  $\pm 1$  standard deviation are presented in results. Error bars in x-axis data are presented to show measurement points before and after tool wear inspection points ( $\pm 0.1125$  m).

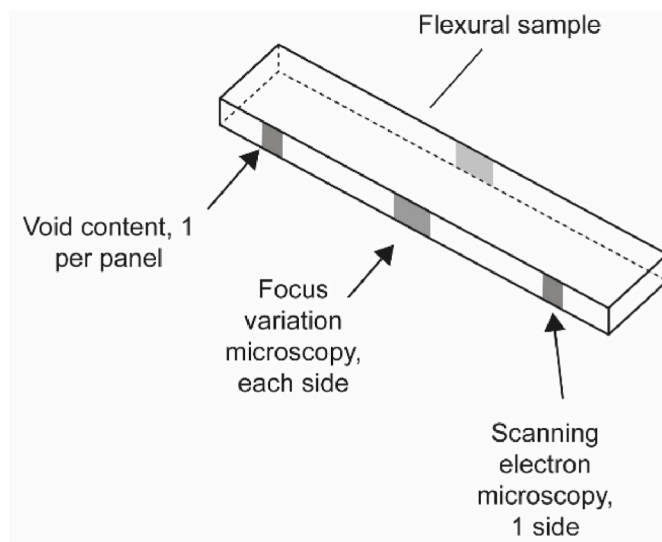


Fig. 4. Post machining assessment locations for individual mechanical test coupons (SEM shown in supplementary information).

## 2.4. Flexural testing

Upon completion of post-machining surface inspection, four point bend testing, for the 4 samples associated with each tool wear inspection points given in Table 2, was tested as per ASTM D6272 [31]. Flexural testing has been chosen due to its efficacy to show links between machined edge quality and mechanical strength [18,20,32], A Tinius Olsen H5K-T tensile/compression rig was used with a Tinius Olsen 500LC laser extensometer to determine mid-point deflection with a one half support span used to ensure maximum shear between the two loading noses. Flexural modulus was taken as an average of five gradients from the load-displacement curve with individual crosshead rates calculated for each sample (average width and thickness taken from 3 measurements per sample). Load cell and laser extensometer calibrations result in a  $\pm 1.47\%$  error for flexural strength results.

## 3. Results and discussion

### 3.1. Characterisation of CFRP materials

Tg results obtained through DMA provides an average Tg value of  $115.38 \pm 0.70$  °C across all panels used, with the low standard deviation suggesting a robust manufacturing methodology. DSC analysis shows an average cure of  $99.99 \pm 0.001\%$  which shows the DGEBF has freely reacted with the TETA hardener and tool wear will not be influenced by degree of cure changes across different wear panels.

Optical analysis of panels used in flexural strength testing shows an average and standard deviation void content of  $0.17 \pm 0.05\%$ . The low void content value, typical of the RTM process, to minimise the influence on final mechanical strength, allowing surface quality to be the dominating factor.

Geometric analysis has shown that of the 60 samples used for flexural testing, the average thickness of the samples was  $3.06 \pm 0.047$  mm. The average width of the trimmed samples was  $12.60 \pm 0.061$  mm. The tolerance is taken from the standard deviation of the samples.

### 3.2. Wear assessment

The results of tool wear inspection are shown in Fig. 5. It can be seen that the uncoated tool wears rapidly compared to the coated tool, in line with expectations [3], as the carbide edge is quickly worn away by the abrasive fibres. Whilst the uncoated tools show an overall upward trend in  $\Delta ER$ , the rate of wear is much smaller for the coated tool, suggesting it is more durable, in line with expectations. Whilst an upward trend of overall wear is observed, there are some instances for both tools where



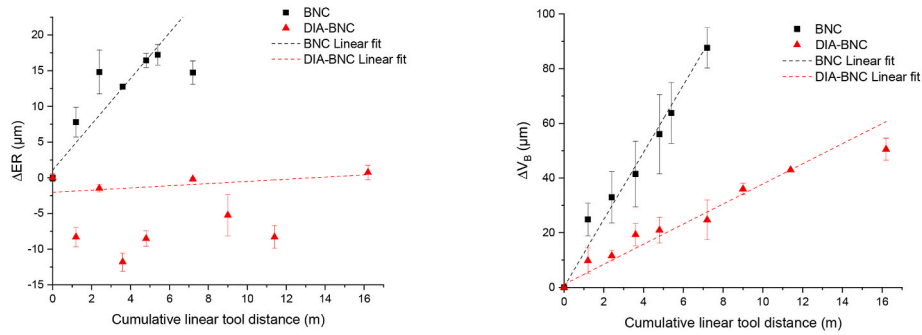


Fig. 5. a)  $\Delta ER$  and b)  $\Delta V_B$  for BNC and DIA-BNC tools.

the edge radius becomes sharper, particularly for the DIA-BNC tool. Whilst expected initially due to the coating process providing a large edge radius compared to the uncoated tool ( $16.64 \pm 0.58$  versus  $6.08 \pm 0.49 \mu\text{m}$  for DIA-BNC and BNC, respectively), allowing for the coating to be preferentially worn away, the tool continues to dull and sharpen throughout the 16.2 m tested. This was an unexpected result as it was anticipated that the edge radius would only increase after an initially bedding in period. That this appears to be happening more frequently than the uncoated tools suggests that the diamond layers that form the coating are able to slip over each other/shed to allow this process to occur quickly [33].

Vaughn [34] notes that tool wear occurs initially at a rapid rate before steady state and final tool failure. Whilst an initial high wear period can be seen for the uncoated tool up to 2.4 m, for the  $ER$  metric in particular, this is not as apparent for the coated tool. For both tool instances, the tool does not appear to have reached the end of its life which is normally attributed to a significant acceleration of flank wear [35] which may limit the observed differences in mechanical strength.

Comparing the ubiquitous  $V_B$  measurement against the more recent  $ER$  method, it can be stated that both offer a useful metric for tool wear. However, whilst  $V_B$  is a convenient method to assess tool wear for CFRP milling tools, it does not assess the actual cutting nose where the cutting mechanisms take place. The edge rounding method suggested by Faraz et al. [14] has been applied to milling tools with satisfactory results that highlight the ever changing nature of the cutting edge, which constantly sharpens and dulls.

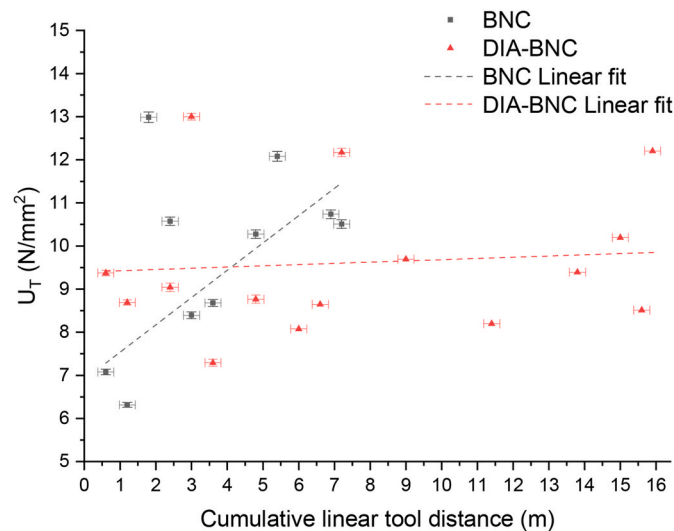


Fig. 6. Overall  $U_T$  versus cutting distance for BNC and DIA-BNC tool with linear fit to show general upward trend of  $U_T$  for increasing amounts of tool wear.

### 3.3. Dynamometer assessment

Fig. 6 shows the results of  $U_T$  for specified tool wear points. Whilst there is a general upward trend of  $U_T$ , suggesting that tool wear has occurred and meeting the expectation that worn tools produce higher cutting forces due to less edge acuity, there is a large fluctuation of  $U_T$  which is unexpected. Whilst the variation is unexpected, Engdahl [33] notes that CVD drilling tools produce a similar fluctuation in thrust force. This suggests that the tool geometry is wearing in such a way that forces increase and decrease throughout tool life.

The fluctuation in  $U_T$  results can be explained by comparing values to the cutting edge radius,  $ER$  which shows a cutting edge that continually cycles through a dulling and sharpening phase. It is therefore postulated that the cutting edge radius changes proportionally with  $U_T$  with a comparison, shown in Fig. 7 for a small section of cutting indicating a shared trend.

A proportionality test between  $U_T$  and  $ER$  values for each tool wear inspection point has been completed to determine if the difference between data points is constant, with results shown in Table 4. The proportionality between the two datasets is relatively constant and the small standard deviations of proportionality for the uncoated tool in particular suggests that the two trends ( $U_T$  and edge radius) are related. Analysis of covariance (ANCOVA) has been completed to supplement the proportionality data. This utilises linear regression fits through the  $U_T$  and edge radius data with respect to cumulative linear tool distance. Whilst the fits have differing Y intercept points due to the nature of having two different Y measurements, the slope of these regression fits can be compared to see if they are statistically different from each other. In this case the null hypothesis states that the slope of the two lines are not statistically different [36]. ANCOVA analysis has been completed in Minitab by stipulating a condition interaction term between  $U_T$  and edge radius in a standard fitted linear regression model. Through ANCOVA, with a significance level of 95 %, a comparison of two gradients yields a p-value  $> .05$  for both tools. This requires the null hypothesis to be accepted, i.e. there is no statistical difference between the slopes of the two fitted regression lines for  $U_T$  and edge radius. This elucidates that  $U_T$  and edge radius conditions follow the same trend for the cumulative linear tool distance input. All results shown in Table 4 show that there is a link between cutting forces, in this case measured as  $U_T$ , and edge radius,  $ER$ , which has previously not been shown within literature for CFRP edge trimming processes for non-orthogonal CVD coated tooling.

### 3.4. Post machining surface assessment

#### 3.4.1. Focus variation assessment

The results of  $S_a$  plotted against cumulative linear tool distance, Fig. 8, show a general increase with tool wear for the BNC tool and the inverse, a decrease of  $S_a$  with DIA-BNC tool wear. It is also noted that  $S_a$  appears to both increase and decrease as cumulative linear tool distance increases. Whilst this does not meet with an expectation that  $S_a$  should always increase with tool wear, it is noted in Duboust et al. [8] and

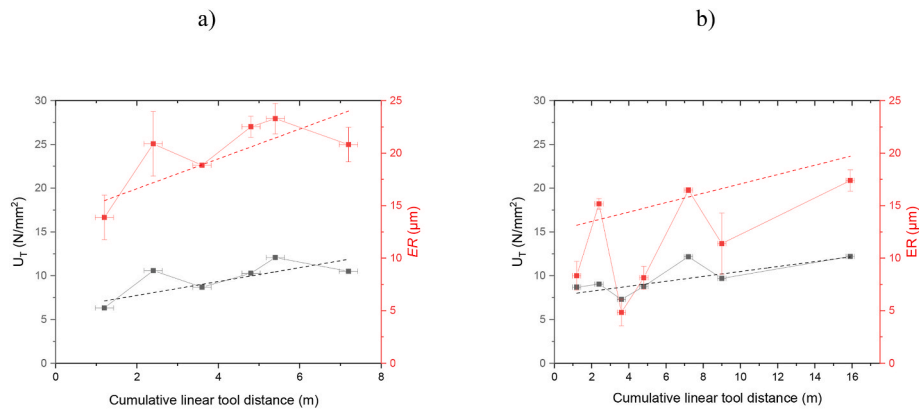


Fig. 7.  $U_T$  and cutting edge radius plots for a) BNC and b) DIA-BNC with linear regression fits to  $U_T$  and  $ER$  data for the purposes of ANCOVA slope comparison.

Table 4

Proportionality of  $U_T$  and edge radius data and ANCOVA p-value results for comparison of linear regression fitted lines for  $U_T$  and edge radius data (bold, italic = significant).

Tool	Average proportionality	Standard deviation of proportionality	ANCOVA p-value
BNC	2.07	0.12	.511
DIA-BNC	1.07	0.22	.441

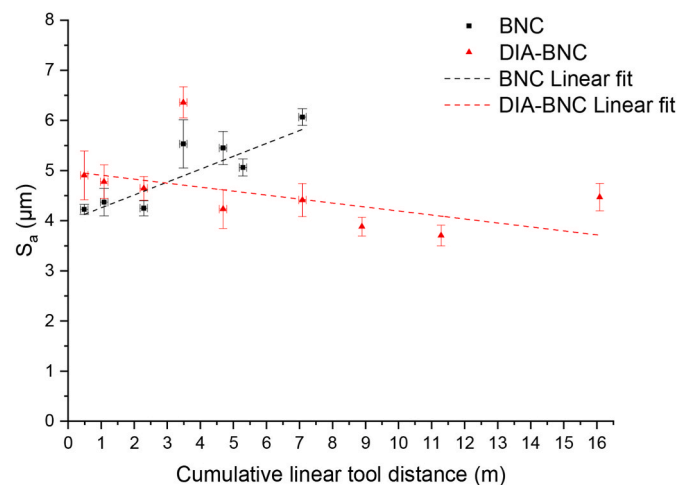


Fig. 8. Average  $S_a$  values for surfaces machined with BNC and DIA-BNC, highlighting the variable nature of  $S_a$  with an overall trend of increased  $S_a$  for increased tool wear.

Sheikh-Ahmad and Sridhar [37] tool wear trials that  $S_a$  does not always increase linearly, and indeed  $S_a$  can decrease as the cutting distance increases. The observation of a non-linear trend in this data set is exacerbated by the increase in inspection points where distances between CFRP surface measurements as little as 375 mm have been completed whilst it is known that  $ER$  is constantly varying. As literature typically uses larger inspection points [8,37], where  $ER$  increases and does not vary, as seen in Fig. 5, this trend may not have been observed before.

In addition to areal metrics, there is an observable difference in surface topography for CFRP coupons edge trimmed with uncoated tools at the start and end of the tool wear trial, as shown in Fig. 9. The surface topography at the start of tool life matches expectations [18,20], as it is dominated by fibres orientated at  $-45^\circ$  to the cutting edge, observed as large gouges/areas of fibre pull-out where the cutting mechanism

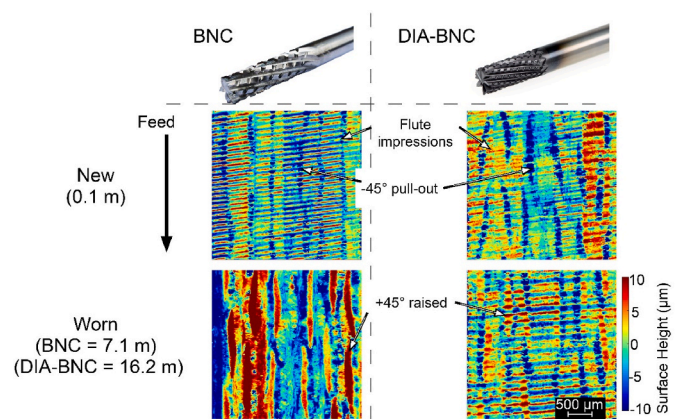


Fig. 9. Surface height topography at start and end of coated and uncoated BNC and MFC tool life, noting surface defects caused by differing fibre orientations to the cutting edge.

removes whole tows of fibre material. With increasing tool wear for the BNC tool, the cutting mechanism changes significantly such that the  $45^\circ$  fibres protrude from the surface. This suggests that significant spring back has occurred where the cutting edge is unable to shear the fibres; instead the fibres are pushed beneath the cutting edge and spring back as the tooth passes, in line with literature [38–40] and in particular that of Giroi et al. [41] who note that a low edge acuity produces significant spring back of  $45^\circ$  fibres. This has not been previously reported using focus variation methods. Striations on the machined surface are visible in the surface topography of the unworn BNC tool which is not evident in worn tool cases. This could be due to the worn tools generating more heat which subsequently causes additional matrix smearing, thus masking individual teeth grooves. Chatter has been ruled out as the cause of this phenomena with fast Fourier transform (FFT) transformation of dynamometer data showing a dominant frequency at the spindle speed of 8000 rpm.

There appears to be limited difference between the surface topography of coupons machined with the DIA-BNC tool which is expected given the aforementioned low rate of overall tool wear.

Whilst observable topography defects due to tool wear can be seen for the uncoated tools in particular, the correlation of all measured areal metrics (see supplementary data for definitions of all metrics) to tool wear must be considered for each tool. These results will highlight if any metric is able to capture tool wear. The results of linear regression analysis, used due to the appearance of linear trends in all residual data scatterplots, is shown in Fig. 10 a). The results show that, even with the varying dynamometer force noted in Fig. 6, and varying tool wear in terms of  $ER$ , a number of metrics are able to observe changes on the

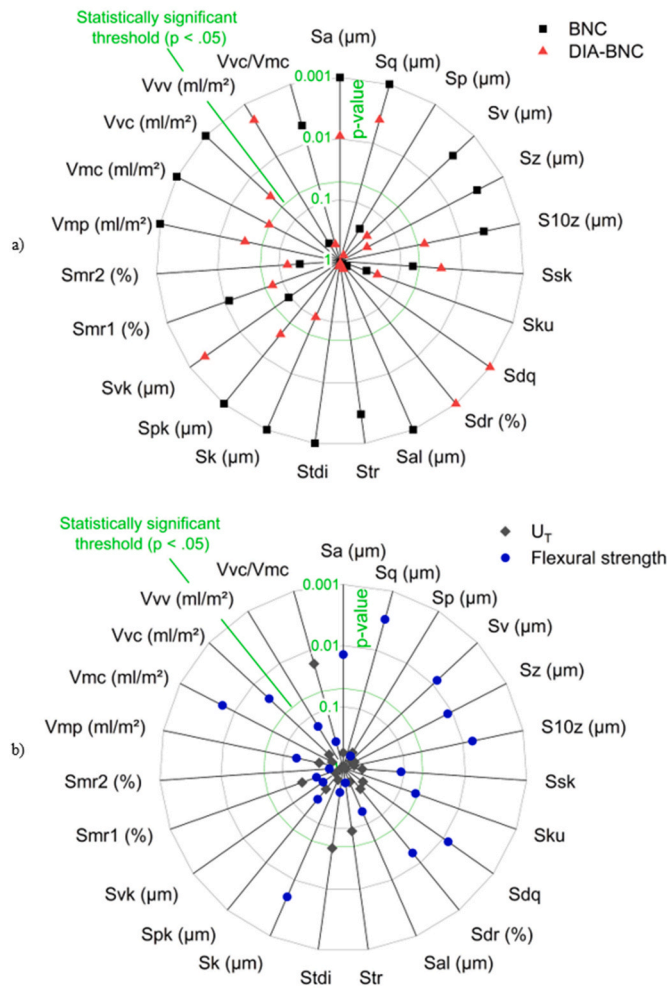


Fig. 10. Radar plot with statistically significant 0.05 threshold showing p-value results for a) correlation of tool wear distance to surface quality metrics for both BNC and DIA-BNC tools and b) correlation of  $U_T$  and flexural strength to surface quality metrics for both BNC.

machined surface with statistical significance. In particular  $S_a$ ,  $S_q$ ,  $S_{10z}$ ,  $S_{pk}$ ,  $V_{mp}$ ,  $V_{mc}$  and  $V_{vc}$ , are metrics that can be used for both tools to determine tool wear. Of the measurement types noted by Blunt and Jiang [42], each sub-set, i.e. amplitude, hybrid, spacing, linear areal material ratio curve, material volume and void volume all show statistical links to tool wear, particularly important for the DIA-BNC tool which saw low amounts of tool wear.

The surface metrics are compared to  $U_T$  for BNC only due to the high amount of wear, with results shown in Fig. 10 b). As only  $S_{tdi}$  and  $V_{vc}/V_{mc}$  are below the statistical threshold of .05 with a 95% confidence interval, the majority of metrics including  $S_a$ , a well-used metric, are  $>0.05$ , the null hypothesis must be accepted i.e. there is no link between  $U_T$  and the majority surface metrics.

### 3.5. Flexural testing results

The results of flexural strength changes for increased tool wear is presented in Fig. 11 with a strength reduction of up to 10.5 % reported for BNC but an increase of up to 2.2 % for the DIA-BNC tool when linear regression models are applied to results. This fits with the expectation that the uncoated tool has worn and produces increased cutting forces (Fig. 6) and statistically different surfaces exist due to wearing of the tool (Figs. 9 and 10 b)). The purpose of the coating has served its purpose in

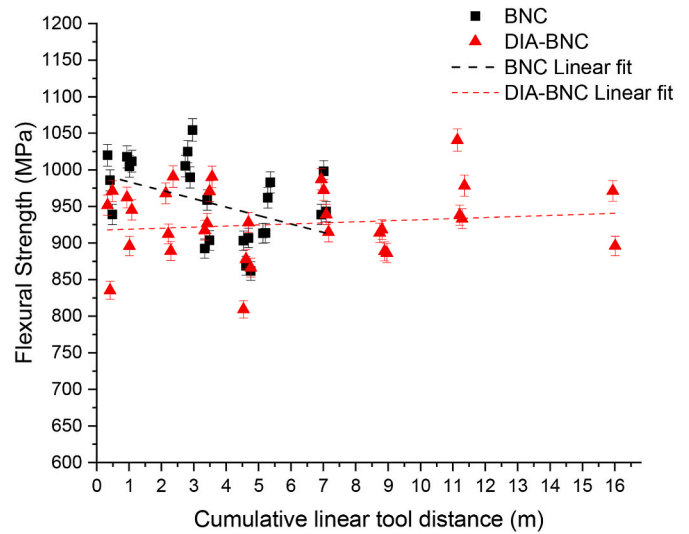


Fig. 11. Flexural strength of coupons machined with BNC and DIA-BNC tools showing decrease and increase in flexural strength for uncoated and coated tools, respectively.

Table 5

Linear regression p-value results for correlation between cumulative linear tool distance and  $U_T$  to flexural strength (bold, italic = significant).

Parameter (Variable)	Regression p-value (cumulative linear tool distance)	
	BNC	DIA-BNC
Flexural strength	<b>.029</b>	.510
Flexural strength	.591	<b>.180</b>

protecting large changes to the cutting edge. The overall minor changes in ER for the coated tool have not provided a sufficient change in surface integrity to affect flexural strength.

Table 5 shows the statistical links between tool wear (as cumulative linear tool distance traversed) and flexural strength for the BNC tool (p-value = .029) whereas the flexural strength of coupons machined with the DIA-BNC tool are not statistically linked to tool wear (p-value = .510). This fits with the knowledge that the tool wear and surface quality changes for the DIA-BNC coated tool is minimal, therefore any change to flexural strength is unlikely.

Fig. 10 b) shows the link between areal surface metrics and flexural strength. Some metrics are statistically linked to flexural strength including  $S_a$ ,  $S_q$ ,  $S_v$ ,  $S_z$ ,  $S_{10z}$ ,  $S_{dq}$ ,  $S_{dr}$ ,  $S_k$ ,  $V_{mc}$  and  $V_{vc}$  for the BNC tool. These metrics could be used as predictors of failure strength in larger parts or used as upper acceptable limits of surface quality in manufacturing specifications.

Table 5 shows the results of final cross correlation where the  $U_T$  response is tested against the variable of flexural strength. It shows that  $U_T$  is not a successful metric to measure flexural strength due to tool wear. It is suggested that the variation of  $U_T$  due to the increase and decrease in cutting edge radius has limited its usefulness to observe flexural strength changes.

## 4. Conclusions

Tool wear is a critical issue in terms of overall part cost and machined quality with little known about the overall effects of tool wear on mechanical performance. This study has investigated the effect of tool wear on flexural strength performance by edge trimming, incorporating ER, a CFRP specific tool wear metric,  $V_B$  wear, correlation to cutting forces through  $U_T$  and areal surface inspection. Based on a rigorous



characterisation and experimental methodology, the following conclusions can be drawn;

- The uncoated carbide tool (BNC) wears more quickly than the diamond CVD coated (DIA-BNC) for both measured metrics,  $V_B$  and  $ER$ . Whilst both tool wear measurements were useful, the  $ER$  metric showed a continual cycling of tool sharpening and dulling which corresponded to measured cutting forces. It is observed that both  $ER$  and  $U_T$  measurements increase and decrease proportionally and that statistical analysis through ANCOVA methods shows that the two metrics are linked.
- Surface topography images and areal metrics imaging show that the uncoated carbide produces different surfaces due to a change in cutting mechanism which is prevalent for fibres at  $45^\circ$  to the cutting edge. The lower acuity edges allow fibres to be pushed beneath the surface instead of the typical shearing process that occurs with high acuity cutting edges.
- Whilst  $ER$  and  $U_T$  metrics could be linked, further links to surface metrics could not be drawn. However, multiple areal metrics were able to show the effects of tool wear with statistical significance ( $S_a$ ,  $S_q$ ,  $S_{10z}$ ,  $S_{pk}$ ,  $V_{mp}$ ,  $V_{mc}$  and  $V_{vvc}$ ) for both tool types. This highlights the efficacy of areal metrics compared to stylus based methods which are sometimes not able to truly represent the surface quality [18,20].
- As tool life has been identified as a critical factor for mechanical performance in terms of flexural strength reductions of up to 10.5%, it is imperative that strict limits are placed on tool life used to machine load bearing structures, e.g. primary aircraft structure, especially when uncoated carbide tools are used to cut material. It was found that the coated tool produced flexural strength values with limited change, indicative of the low amount of wear shown on the cutting edges.

#### Author statement

Sam Ashworth; Writing – Original draft, Methodology, Software, Validation, Formal Analysis, Investigation, Data curation, Conceptualisation. J. Patrick A. Fairclough – Methodology, Resources, Conceptualisation, Supervision, Writing, Review & Editing. Yoshihiro Takikawa – Methodology, Resources, Writing – Review and Editing. James Meredith – Writing – Review & Editing, Funding acquisition. Kevin Kerrigan – Writing – Review & Editing, Funding acquisition, Conceptualisation.

#### Declaration of competing interest

The authors declare that they have no known competing financial interests or personal relationships that could have appeared to influence the work reported in this paper.

#### Acknowledgements

The authors would like to acknowledge the EPSRC Industrial Doctorate Centre in Machining Science (EP/L016257/1) for the funding of this work and to the OSG Corporation for the supply of tools. Thanks are also extended to staff of the Factory of the Future, AMRC.

#### Appendix A. Supplementary data

Supplementary data to this article can be found online at <https://doi.org/10.1016/j.wear.2022.204340>.

#### References

- [1] Boeing Shares Work, but Guards its Secrets, The Seattle Times, 2007.
- [2] M.F. Ashby, Chapter 4 - material property charts, in: M.F. Ashby (Ed.), *Materials Selection in Mechanical Design*, fourth ed., Butterworth-Heinemann, Oxford, 2011, pp. 57–96.
- [3] J. Sheikh-Ahmad, J.P. Davim, Tool wear in machining processes for composites, in: H. Hocheng (Ed.), *Machining Technology for Composite Materials*, Woodhead Publishing, 2012.
- [4] J.Y. Sheikh-Ahmad, M. Dhuttargaon, H. Cheraghi, New tool life criterion for delamination free milling of CFRP, *Int. J. Adv. Manuf. Technol.* 92 (5) (2017) 2131–2143.
- [5] K. Sauer, M. Witt, M. Putz, Influence of cutting edge radius on process forces in orthogonal machining of carbon fibre reinforced plastics (CFRP), *Proced. CIRP 85* (2019) 218–223.
- [6] N. Geier, J. Xu, C. Pereszlai, D.I. Poór, J.P. Davim, Drilling of carbon fibre reinforced polymer (CFRP) composites: difficulties, challenges and expectations, *Procedia Manuf.* 54 (2021) 284–289.
- [7] D.I. Poór, N. Geier, C. Pereszlai, J. Xu, A critical review of the drilling of CFRP composites: burr formation, characterisation and challenges, *Compos. B Eng.* 223 (2021), 109155.
- [8] N. Duboust, D. Melis, C. Pinna, H. Ghadbeigi, A. Collis, S. Ayvar-Soberanis, et al., Machining of carbon fibre: optical surface damage characterisation and tool wear study, *Proced. CIRP 45* (2016) 71–74.
- [9] W. Xu, L. Zhang, Tool wear and its effect on the surface integrity in the machining of fibre-reinforced polymer composites, *Compos. Struct.* 188 (2018) 257–265.
- [10] J. Sheikh-Ahmad, Chapter 4 Tool Materials and Wear. *Machining of Polymer Composites*, Springer, 2008.
- [11] S. Swan, M.S. Bin Abdullah, D. Kim, D. Nguyen, P. Kwon, Tool wear of advanced coated tools in drilling of CFRP, *J. Manuf. Sci. Eng.* 140 (11) (2018).
- [12] Corporation O. OSG Aerospace Solutions - Composite. *Aerospace Solutions - Composite2014*. p. 54.
- [13] ISO, Tool Life Testing in Milling - Part 2: End Milling, 1988. ISO 8688-2:1989.
- [14] A. Faraz, D. Biermann, K. Weinert, Cutting edge rounding: an innovative tool wear criterion in drilling CFRP composite laminates, *Int. J. Mach. Tool Manuf.* 49 (15) (2009) 1185–1196.
- [15] N. Duboust, C. Pinna, H. Ghadbeigi, A. Collis, S. Ayvar-Soberanis, K. Kerrigan, et al., FE modelling of CFRP machining- prediction of the effects of cutting edge rounding, *Proced. CIRP 82* (2019) 59–64.
- [16] N. Duboust, M. Watson, M. Marshall, G.E. O'Donnel, K. Kerrigan, Towards intelligent CFRP composite machining: surface analysis methods and statistical data analysis of machined fibre laminate surfaces, *Proc. IME B J. Eng. Manufact.* (2020), 95440542096092.
- [17] W. Hintze, D. Hartmann, C. Schütte, Occurrence and propagation of delamination during the machining of carbon fibre reinforced plastics (CFRPs) – an experimental study, *Compos. Sci. Technol.* 71 (15) (2011) 1719–1726.
- [18] S. Ashworth, J.P.A. Fairclough, A.R.C. Sharman, J. Meredith, Y. Takikawa, R. Scaife, et al., Varying CFRP workpiece temperature during slotting: effects on surface metrics, cutting forces and chip geometry, *Proced. CIRP 85* (2019) 37–42.
- [19] M. Haddad, R. Zitoun, H. Bougherara, F. Eyma, B. Castanié, Study of trimming damages of CFRP structures in function of the machining processes and their impact on the mechanical behavior, *Compos. B Eng.* 57 (2014) 136–143.
- [20] S. Ashworth, J.P.A. Fairclough, Y. Takikawa, R. Scaife, H. Ghadbeigi, K. Kerrigan, et al., Effects of machine stiffness and cutting tool design on the surface quality and flexural strength of edge trimmed carbon fibre reinforced polymers, *Compos. Appl. Sci. Manuf.* 119 (2019) 88–100.
- [21] M. Monoranu, S. Ashworth, R. M'Saoubi, J.P. Fairclough, K. Kerrigan, R.J. Scaife, et al., A comparative study of the effects of milling and abrasive water jet cutting on flexural performance of CFRP, *Proced. CIRP 85* (2019) 277–283.
- [22] A.H. Sheikh-Ahmad, Effect of edge trimming on failure stress of carbon fibre polymer composites, *Mach. Machinab. Mater.* 13 (2/3) (2013).
- [23] M. Haddad, R. Zitoun, F. Eyma, B. Castanie, Study of the surface defects and dust generated during trimming of CFRP: influence of tool geometry, machining parameters and cutting speed range, *Compos. Appl. Sci. Manuf.* 66 (2014) 142–154.
- [24] N. Nguyen-Dinh, R. Zitoun, C. Bouvet, S. Leroux, Surface integrity while trimming of composite structures: X-ray tomography analysis, *Compos. Struct.* 210 (2019) 735–746.
- [25] F.-J. Wang, J.-W. Yin, J.-W. Ma, Z.-Y. Jia, F. Yang, B. Niu, Effects of cutting edge radius and fiber cutting angle on the cutting-induced surface damage in machining of unidirectional CFRP composite laminates, *Int. J. Adv. Manuf. Technol.* 91 (9–12) (2017) 3107–3120.
- [26] A. Hejjaji, R. Zitoun, L. Crouzeix, S.L. Roux, F. Collombet, Surface and machining induced damage characterization of abrasive water jet milled carbon/epoxy composite specimens and their impact on tensile behavior, *Wear* 376–377 (2017) 1356–1364.
- [27] A. Hejjaji, R. Zitoun, L. Toubal, L. Crouzeix, F. Collombet, Influence of controlled depth abrasive water jet milling on the fatigue behavior of carbon/epoxy composites, *Compos. Appl. Sci. Manuf.* 121 (2019) 397–410.

- [28] N. Nguyen-Dinh, C. Bouvet, R. Zitoune, Influence of machining damage generated during trimming of CFRP composite on the compressive strength, *J. Compos. Mater.* (2019).
- [29] K. Kerrigan, G.E. O'Donnell, On the relationship between cutting temperature and workpiece polymer degradation during CFRP edge trimming, *Proced. CIRP* 55 (2016) 170–175.
- [30] S. Ashworth, J. Rongong, P. Wilson, J. Meredith, Mechanical and damping properties of resin transfer moulded jute-carbon hybrid composites, *Compos. B Eng.* 105 (2016) 60–66.
- [31] ASTM, Standard Test Method for Flexural Properties of Unreinforced and Reinforced Plastics and Electrical Insulating Materials by Four-Point Bending, ASTM D6272, 2010.
- [32] D. Arola, M. Ramulu, Net-shape machining and the process-dependent failure of fiber-reinforced plastics under static loads, *J. Compos. Technol. Res.* 20 (4) (1998) 210–220.
- [33] N.C. Engdahl, CVD diamond coated rotating tools for composite machining, *SAE Int.* (2006).
- [34] R.L. Vaughn, Modern metals machining technology, *J. Eng. Ind.* 88 (1) (1966) 65–71.
- [35] K. Kerrigan, R.J. Scaife, Wet vs dry CFRP drilling: influence of cutting fluid on tool performance, *Proced. CIRP* 77 (2018) 315–319.
- [36] Minitab, How to Compare Regression Slopes, 2016.
- [37] J. Sheikh-Ahmad, G. Sridhar, Edge trimming of CFRP composites with diamond coated tools: edge wear and surface characteristics, *SAE Tech. Pap.* (2002).
- [38] D.H. Wang, M. Ramulu, D. Arola, Orthogonal cutting mechanisms of graphite/epoxy composite. Part II: multi-directional laminate, *Int. J. Mach. Tool Manufact.* 35 (12) (1995) 1639–1648.
- [39] D.H. Wang, M. Ramulu, D. Arola, Orthogonal cutting mechanisms of graphite/epoxy composite. Part I: unidirectional laminate, *Int. J. Mach. Tool Manufact.* 35 (12) (1995) 1623–1638.
- [40] X.M. Wang, L.C. Zhang, An experimental investigation into the orthogonal cutting of unidirectional fibre reinforced plastics, *Int. J. Mach. Tool Manufact.* 43 (10) (2003) 1015–1022.
- [41] F. Giro, L.N. Lopez De Lacalle, A. Lamikiz, D. Iliescu, M.E. Gutierrez, Machinability aspects of polymer matrix composites, in: J.P. Davim (Ed.), *Machining Composite Materials*, ISTE Ltd and John Wiley & Sons Ltd., 2010.
- [42] L. Blunt, X. Jiang, 2 - Numerical Parameters for Characterisation of Topography. *Advanced Techniques for Assessment Surface Topography*, Kogan Page Science, Oxford, 2003, pp. 17–41.